C. P. No. 527

(21, 591)

A.R.C. Technical Report

C. P. No. 527

(21, 591)

A.R.C. Technical Report

MINISTRY OF AVIATION

AERONAUTICAL RESEARCH COUNCIL

CURRENT PAPERS

An Experimental Investigation of Cavitation Inception in the Rotor Blade Tip Region of an Axial Flow Pump

by

A. B. Mitchell

An Experimental Investigation of Cavitation Inception in the
Rotor Blade Tip Region of an Axial Flow Pump*
- By -
A. B. Mitchell

Abstract

The variation of tip clearance cavitation number with both tip clearance and flow coefficient in a single stage axial flow pump has been studied experimentally. It is shown that there exists a critical tip clearance below which surface cavitation at the blade tip occurs first and above which vortex cavitation due to the clearance flow occurs first. In general, the tip clearance cavitation number is a minimum at this critical tip clearance so that in a properly designed pump, i.e., one with maximum cavitation - free performance, tip clearance and blade surface cavitation number are synonymous.

Introduction

1. There are, in general, two possible sources of cavitation due to the internal flow patterns of an axial flow pump, and it is necessary in the design of such units to be able to predict the onset of both types. The first, and perhaps simpler, type is the familiar blade surface cavitation. Although the onset of blade surface cavitation is affected by secondary flows, i.e., three-dimensional flows, in the machine it is largely determined by the main flow and present design methods and data are sufficient to allow a reasonably accurate prediction.

2. The second type of cavitation is associated with the flow that takes place in the clearance between the rotor blade tip and the pump casing, from the high pressure surface of the rotor blade to the low pressure surface. Similar flows could, of course, exist between the tips of the stator blades and inlet guide vanes - if fitted - and the pump casing. Usually, however, the mechanical design is simplified when these blades are fixed to the casing and hub and no clearance exists for the flows to take place. Even in the few cases where clearances do exist, the calculation of tip flows is simplified due to the absence of relative motion between the blades and the casing. The present investigations of rotor blade tip flows only, therefore, may be expected to throw considerable light on them as well.

3. Although tip clearance cavitation has been known for many years to cause a great deal of erosion in axial flow pumps, little is known of how its inception point varies with variation of design parameters. This is probably due to its dependence mainly on secondary flows which present design methods do not even pretend to take into account. In spite of recent American work which has indicated the existence of an optimum tip clearance for a minimum tip clearance cavitation number, the choice of tip clearance used in a particular design is usually dictated by other factors than cavitation due to lack of sufficient design data. It is usual to find, therefore, that in most axial flow pumps, tip clearance cavitation occurs long before blade surface cavitation and this tendency has been emphasised in recent years by improved methods of blade design.

4./

---

*Previously issued as A.R.L./R1/G/HY/11/2 - A.R.C.21,591.

4. Since tip clearance cavitation might possibly set a limit on the cavitation - free performance of axial flow pumps, an initial experimental investigation has been carried out with three objectives in mind:-

(i) To investigate the variation of tip clearance cavitation number with other parameters such as clearance distance and flow coefficient for a particular design.

(ii) For a particular design to determine the relative values of tip clearance cavitation number and blade surface cavitation number and to obtain guidance on the more promising methods of reducing - if necessary - the former.

(iii) To obtain sufficient information on the mechanism of tip clearance cavitation on which to base a theoretical approach.

5. This report presents the results of this experimental programme. In spite of the preliminary nature of this work it was felt that the results were of sufficient interest to justify publication at this stage.

Experimental Equipment

6. The axial flow pump test rig used in the experimental investigation is shown in Fig.1 and was designed so that it could be inserted into the A.R.L. 12 in. water tunnel in place of the conventional working section. To accommodate the greater length of the test rig, part of the tunnel diffuser was also replaced with a shorter length. As it was intended to operate the pump over a large range of flow coefficients both above and below the design value a variable throttle was introduced into the tunnel circuit at the downstream end of the new diffuser length. This consisted of two perforated plates which could be rotated relative to one another from outside the tunnel. The system worked satisfactorily except at low tunnel pressures when it was found impossible to seal the gland round the external adjusting screw. Air leaking into the tunnel at this position found its way to the working section and gave false indications of cavitation. Eventually, therefore, the external adjustment was removed, the throttle set in a fixed position to give a fixed pressure drop and final adjustment of the pressure loss round the tunnel circuit achieved by running the main tunnel impeller either forwards or backwards.

7. The axial flow pump test rig itself (Fig.1) has a hub to tip diameter ratio of 0.5 with a constant hub diameter of 6 in. The power input to the rotor blades is through an inclined shaft from a 30 H.P., three phase, variable speed A.C. motor mounted externally to the tunnel. A 2 to 1 speed reduction gearbox also mounted externally allows the pump speed to be continuously variable between 375 and 750 R.P.M. Strain gauge torque gauges and sliprings mounted on the pump end of the input drive shaft together with yawmeters and provision for inserting the yawmeters through the outer casing enable the overall blading characteristics to be obtained. In the present series of tests, however, these facilities were not used. There are also a number of static pressure holes both upstream and downstream of the blades in the stationary portions of the hub. Viewing ports of perspex are placed in suitable positions in the external casing to allow visual investigations of conditions at the rotor blade tips.

8. The test rig is capable of containing up to two complete stages of blading plus an inlet guide vane row, i.e., guide vane row, rotor row, stator row, rotor row and stator row. Any of these blade rows not required can be removed and making-up pieces inserted into the root slots to obtain continuity of water flow surface. In the present experiments a single stage only consisting of a rotor and stator row were used. The rotor row contained thirteen blades and the stator row fourteen.

9. The blading design of this single stage is what is commonly called "free vortex", i.e., the outlet whirl velocity from the rotor blades is made

to/

to vary inversely as the radius. The main characteristics of the blades are given in Tables I and II and were derived on the basis of the methods and data given in Refs.2, 3, 4 and 5. The N.G.T.E. C.5 base profile was used for both rotor and stator blades. No measurements of overall stage characteristics have been made as these were not required for the present programme although measurements of pressure rise across the rotor blades, as discussed later, and shown in Fig.10 were made.

10. The blades were manufactured in bronze by means of a precision moulding and casting technique from a hand-made master blade. Although in the blades produced, the important dimensions of the tip sections were within the tolerances specified, the surface finish was disappointing and in some cases the leading edge radius had to be dressed by hand. A few of the better blades were selected on which to carry out the experimental observations and it is felt that different performances due to slightly differing profiles etc. is negligible and certainly within the other experimental errors. Originally the blades on which the measurements were made had sharp corners at the tip on both the pressure and suction surfaces. Initial tests showed inconsistent cavitation performance on some blades due to slight burrs at the junction of the tip and pressure surfaces which caused separation of the flow in the tip clearance. Throughout the final tests, therefore, a radius approximately equal to the tip clearance was used in the corner between the tip and pressure surfaces of the blades.

Measurements and Procedure

11. The general procedure was to pre-set R.P.M. accurately and mass flow coefficient approximately and then for various blades of different tip clearances to determine the tip cavitation inception number.

12. **Mass Flow Coefficient** (V_a/U_m) The pump has been designed for a mass flow coefficient of 0.80 and the investigations were carried out for different values between 0.7 and 0.9 and in the main at 0.7, 0.75, 0.80, 0.85 and 0.90. The mean radius blade speed (U_m) was obtained from frequent measurements of R.P.M. of the driving motor by means of a Hasler tachometer. The tachometer was checked before and after the tests in the speed range used and was found to be well within $\pm\frac{1}{2}\%$. Variations in speed of the motor during a run were found to be negligible.

13. The mean axial velocity, V_a, was obtained from the pressure drop across the tunnel contraction. The necessary calibration factors were obtained by running the tunnel without blades in the pump and taking velocity traverses in the region of the leading edge of the rotor blades together with the pressure drop across the tunnel nozzle. As the "free vortex" design assumes a constant inlet axial velocity to the rotor blades independent of radius, the corresponding values of V_a against nozzle pressure drop were obtained by integrating the velocity traverses to get mass flow and then dividing by the pump cross-sectional area. Thus V_a could not be pre-set accurately and the values of flow coefficient aimed at could only be obtained approximately.

14. **Cavitation Inception** All measurements of the cavitation inception point were determined visually. A micro-switch on the drive shaft triggered off a five micro-second duration flash each time a particular rotor blade passed the observation window. The definition of the inception point decided on was the highest pressure at which it was judged by eye that there was at least some cavitation present each time the blade passed the window. The procedure finally adopted was to set the tunnel and pump conditions for a particular flow coefficient and then gradually reduce the tunnel static pressure. The static pressure and other readings were taken when it was judged that some cavitation was present each revolution. For each point the procedure was repeated at least three times and the average value taken as the correct one. In a large number of cases the repeat readings were very close and in no case did the scatter of readings exceed about $\pm10\%$ when expressed as a cavitation inception number.

15. To record the type of cavitation occurring, photographs were taken at the inception point for some conditions using a flash of two micro-second duration. Although cavitation appeared to be fairly continuous when viewed by eye, sometimes only about one photograph in six showed any sign of cavitation at all. When the flash duration was increased to about fifteen micro-seconds, three or four frames in six showed signs of cavitation. This discrepancy between the eye and the camera is presumably due to the retentive powers of the former and is a reminder of the indefinite meaning of the word "inception" particularly when the cavitation takes place in regions of unsteady or turbulent flow. These discrepancies which are no more than a function of the sensitivity of the instruments would, of course, be present to differing degrees in whatever method was chosen to determine the inception point. It was felt, therefore, that even if visual determination of inception has little meaning theoretically, then so have the others and there is little to choose between them from the point of view of theoretical evaluation, provided the method chosen allows consistent results to be obtained.

16. Throughout the cavitation measurements a check on the air content of the tunnel water was kept by means of the A.R.L. Air Content Meter. This remained at 16 c.c. per litre ± 1 c.c. per litre. The temperature of the water was kept between 18 and 20 degrees centigrade.

17. **Tip Clearance** The tip clearances investigated were 0.0055, 0.010, 0.018, 0.026, 0.039 and 0.057 in. These correspond to dimensionless values of λ - tip clearance divided by maximum thickness of the tip section - of 0.0378, 0.0688, 0.124, 0.179, 0.268 and 0.392. These clearances were set on preselected blades so that rapid comparison of cavitation on different blades could be made without altering any conditions except switching the stroboscope from one to another.

18. **Boundary Layer** Measurements of the velocity profile in the wall boundary layer were made with a small pitot tube situated approximately 1/4 in. upstream of the leading edge of the rotor blades. The dimensions of the pitot tube are shown in Fig.2. Although the effect of the velocity gradient on the pitot tube measurements will be to displace the effective measuring point away from the geometric centre of the tube no allowance will be made as the magnitude of the correction required is uncertain.

19. **Pressure Rise Across Rotor Blades** Six static pressure tappings along the casing of the tip of the rotor blades were used to measure the static pressure rise across the rotor blades at the tips. As in the case of the boundary layer velocity measurements, the readings obtained are some kind of average of the periodic fluctuations that must occur as each blade passes the measuring station.

Test Results

20. The results of the cavitation inception measurements at varying values of tip clearance, pump rotational speed and flow coefficient are given in Table III. Also given in the table are the corresponding cavitation inception numbers (K_{va}) based on the mean axial flow velocity at inlet to the rotor blades. The results given in Table III are plotted in Figs.3, 4, 5, 6, 7 and 8, in the form of flow coefficient V_a/U_m, against cavitation inception number, K_{va}, for each value of non-dimensional tip clearance, λ. The photographs of the cavitation at various inception points are shown in Fig.14.

21. The wall boundary layer velocity profile obtained is shown in Fig.9. The scatter of results, corresponding to values obtained under different conditions of V_a/U_m and R.P.M., appears to be random and no systematic variation in profile can be detected. The dotted curve given in Fig.9, therefore, is taken as the profile under all test conditions.

22. The static pressure rise across the tips of the rotor blades is shown in Fig.10 for flow coefficients of 0.7, 0.8 and 0.9. The effect of varying pump R.P.M. on the curves for constant flow coefficient appears to be well within the experimental accuracy.

Discussion/

Discussion of Results

23. Since λ and R.P.M. are precisely specified, the data of Table III are most conveniently plotted in the form of flow coefficient against cavitation number for various values of λ and R.P.M. This is done in Figs.3 to 8 and it is immediately seen that this is not an ideal form for discussion. However, the curves do show some variations with pump R.P.M. under otherwise similar conditions and undoubtedly some of these variations must be due to changes of Reynolds number. But in the majority of cases, particularly at the higher flow coefficients and larger tip clearances, the variations are small and almost within the estimated experimental error. There are, however, two much larger variations. The first is the 600 R.P.M. point at a flow coefficient of 0.7 at the smallest tip clearance (Fig.3) and the second is the 750 R.P.M. point at a flow coefficient of 0.75 at the next to smallest tip clearance (Fig.4). It is significant that these larger variations only appear at the higher incidences - low flow coefficients - and lower clearances and where, as discussed later, cavitation is first due to blade surface cavitation. Again, as discussed later, there is evidence of separation causing the increase in cavitation number at low flow coefficients from Fig.3 to Fig.4 and it seems probable that these two large variations are the combined results of changes of Reynolds number, flow incidence, and boundary layer turbulence etc. on the separation or otherwise of the flow round the tip section.

24. To facilitate discussion, Figs.3 to 8 with some smoothing - have been used to obtain interpolated values of cavitation numbers at flow coefficients of 0.7, 0.75, 0.8, 0.85 and 0.9. The results are plotted in Figs.11, 12 and 13 as cavitation number against dimensionless tip clearance for constant values of flow coefficient. The shapes of the three figures obtained for 600, 675 and 750 R.P.M. are very similar and only relatively minor differences in magnitude exist between them, due to the Reynolds number effects and/or experimental errors mentioned in the previous paragraph. The figures show a startling variation of cavitation number with tip clearance particularly at the low values of flow coefficient. They also show that except possibly for values of flow coefficients above 0.9 there is an optimum value of tip clearance for maximum cavitation resistance. The non-dimensional value of this optimum tip clearance appears to lie between about 0.09 and 0.105 and agrees very closely with the value of 0.1 obtained in Ref.2.

25. The shape of the curves in Figs.11 to 13 must be explainable in terms of variations of static pressure in the pump blade tip region relative to the free stream static pressure. These variations, and hence variations in cavitation number are determined by the total effect of three main factors which are to some extent interdependent. These are:-

(i) Tip incidence.

(ii) Tip clearance flow velocity.

(iii) Static pressure rise through the blade row.

Before a qualitative explanation of these curves is attempted it will be necessary to examine separately and in greater detail the behaviour of each of these three main factors.

26. **Tip incidence** The incidence of the main flow on to the tip section of the blade will largely determine the magnitude and position along the chord of the minimum pressure coefficient of the tip profile. In general, an increase in incidence, i.e., an increase in the angle between the relative flow direction and the tangent to the blade camber line at the leading edge, will decrease the minimum pressure coefficient and move its position towards the leading edge. A decrease in incidence will do the reverse.

27. From the boundary layer traverses shown in Fig.9, it can be seen that the axial velocity at the tip is well below the free stream value even for the largest tip clearances investigated and falls off further with decreasing tip clearance. As the blade tip speed alters only a negligibly small amount with

tip clearance, the flow incidence will increase as the axial velocity decreases, i.e., as the tip clearance decreases. Similarly in each of the Figs.11, 12 and 13, R.P.M. is constant so that reduction of flow coefficient (V_a/U_m) means a reduction of axial velocity and hence an increase of flow incidence to the tip of the blade. In Figs.11 to 13, it should be borne in mind, therefore, that tip incidence increases with decreasing values of V_a/U_m and along lines of constant V_a/U_m, tip incidence increases with decreasing tip clearance.

28. Unfortunately, it is not permissible to calculate the actual magnitude of the tip incidences by means of the boundary layer traverse results, as these measurements are an average value for all blades in the rotor row of which some have different tip clearances. Furthermore, there will be additional local variations in incidence between mid-passage and blade positions. These local variations will be greatly enhanced by the tip clearance flows. The greater the clearance flow velocity, the greater will be the quantity of fluid flowing across the blade tip from the pressure to the suction side. This increased quantity can only be achieved at the expense of some fluid that would otherwise flow completely round the suction side of the profile, without crossing the tip of the blade. The nett result will, therefore, be a local decrease of incidence at the leading edge of the blade tip. Hence the minimum pressure coefficient will always be greater than - but to a varying extent dependent on clearance flow velocities - the values indicated by the two-dimensional argument in para.27 above.

29. Tip clearance flow In the absence of other factors it is to be expected that the magnitude of the tip clearance flow velocity will increase with increasing incidence of the flow to the blade tips, as under these circumstances the pressure difference across the blade tip increases. However, this conclusion is likely to be considerably modified by Reynolds number effects. For values of tip clearance below a certain amount the flow will be increasingly dominated by viscous forces and for tip clearance values above this amount the flow will be increasingly controlled by inertia forces. An experimental determination of this critical Reynolds number was made in Ref.2 for a stationary hydrofoil and the results obtained show that the change from viscous to inertia forces correspond to the region of non-dimensional tip clearance values between about 0.07 and 0.16. For very small tip clearances where incidences are high and therefore large pressure differences exist to produce clearance flows, the resistance to the flow in the clearance is also very high. With the larger tip clearances the incidence is reduced both due to the tip flow itself and also to increased axial velocity; on the other hand the resistance to the flow in the clearance is reduced. It seems likely, therefore, that the magnitude of the tip clearance flow velocity will only increase with increasing incidence down to a tip clearance corresponding to the critical Reynolds number and below which the flow becomes increasingly laminar and the magnitude of the velocity falls off.

30. The clearance flow emerges from the suction side of the blade more or less as a jet which eventually, by interaction with the main flow over the blade suction surface, rolls up to form a vortex of which the core sooner or later cavitates. The strength of the vortex is largely determined by the velocity discontinuity across the jet boundary with the main flow and the core diameter is perhaps largely fixed by the thickness of this surface of discontinuity which in turn will be related to the thickness of the boundary layer on the tip of the blade. Both these factors will determine the cavitation number of the vortex and both alter in such a fashion as to raise the cavitation number, K_{va}, with increasing tip clearance flow velocity.

31. Static pressure rise The static pressure rise through the rotor blade row will also affect the overall cavitation number, K_{va}, because it may modify the magnitude of the chordwise suction distribution obtained from the tip incidence and tip clearance flows. The chordwise static pressure rise shown in Fig.10 is substantially linear but the magnitude is greatly dependent on the flow coefficient. As with the boundary-layer traverses, these measurements are an average for all the blades in the rotor row and undoubtedly the magnitude of the static pressure rise must be reduced with increasing tip clearance. However, over the range of clearances of interest, the variation is probably of no more than a few per cent.

32./

32. During the experimental observations of tip clearance cavitation inception points it was observed that the cavitation appeared first in either one or other of two quite distinct forms. Closer investigation showed that one type always occurred first at the low tip clearance values and the other at the high ones and it was felt that an understanding of the causes of these two different types of cavitation might lead to an explanation of the shapes of the curves in Figs.11 to 13. The most likely explanation of the two forms seems to be that the first is cavitation on the blade surface due to the pressure distribution of the flow around the tip profile and is, therefore, ordinary blade surface cavitation largely dependent on the two-dimensional characteristics of the tip section alone; whereas the second is cavitation in the core of the vortex formed as a result of the interaction of the tip clearance flow and the main flow. To help prove this important point a series of photographs were taken of the cavitation at inception over the whole range of tip clearances and flow coefficients. Although the photographs, shown·in Fig.14, tend to support this hypothesis, their evidence cannot be considered as wholly conclusive as to the origins of the two forms of cavitation. In studying the photographs from this point of view it should be borne in mind that the blade tip is moving relative to the stationary wall boundary layer and that there is, therefore, always a tip flow with a consequent weak vortex even when no clearance flow due to blade pressure difference exists. Some of the cavitation formed on the surface of the blade ahead of the vortex will be swept into it and persist longer there than in the surrounding fluid due to the slightly lower pressure and the vortex core so illuminated will appear to be cavitating. ˙Fig.14(e) is a good example of this. However, in general, if blade surface pressure is the prime cause of cavitation a relatively large lump of cavitation would be expected near the blade surface with the illuminated tail of the vortex sprouting from it but diminishing fairly rapidly. On the other hand where pressure reduction in the cores of the vortex is the prime cause, the cavitation would not be concentrated on the surface of the blade and at the leading edge of the vortex but would rather start thin and thicken up somewhat away from the blade surface. On this basis it appears from the photographs of Fig.14 that for tip clearances below about 0.12 blade surface cavitation always occurs first and for clearances above 0.12 vortex cavitation occurs first. At a clearance of 0.12 sometimes one form of cavitation occurs first and sometimes the other as shown in Figs.14(j) and 14(k).

33. The qualitative effect of the various factors on the cavitation number discussed in the preceding paragraphs can now be added to the photographic evidence to provide an explanation for the shape of the curves in Figs.11, 12 and 13, and this is given below.

(i) At very small tip clearances (λ smaller than about 0.05), separation of the flow from the suction surface causes the initial rise in the curves for a flow coefficient of 0.7 in Figs.11, 12 and 13 and in the 0.75 curve of Fig.13. The flow through the tip clearance is essentially laminar and the velocity small. There is, therefore, very little local decrease of flow incidence and the actual incidence is largely due to the tip being right in the wall boundary layer. Very low minimum pressure coefficients result from the large incidence and blade surface cavitation eventually occurs first. Where the incidences are highest – at the lower values of flow coefficient – separation occurs before cavitation. Cavitation is then delayed somewhat due to an effective improvement of the profile shape. In the absence of separation, K_{va} reduces with reducing incidence, i.e., with increasing tip clearance.

(ii) For values of λ between about 0.05 and 0.08 the velocity through the tip increases as the flow starts to become turbulent. The flow incidence is reduced a little because of the increased flow and also because of the slightly greater boundary layer axial velocity at the tip. The improvement in incidence is sufficient to prevent separation even in the worst case, but the tip flow velocity is still too low to cause vortex cavitation and blade surface cavitation again occurs first.

(iii) For values of λ between about 0.08 and 0.12 the flow through the tip clearance becomes increasingly turbulent and the magnitude of the velocity

increases/

increases as a result.   Incidence again decreases due to increased tip flow
and increased axial velocity at the tip.   Because of the reduced incidence
the suction peak has reduced and moved back along the chord.   Although the
pressure difference across the blade tip has decreased due to decreasing
incidence, there is still a positive increase in tip flow velocity because
of the greatly reduced pressure drop through the tip clearance.   Cavitation
number, K_{va}, has fallen below the values in (i) and (ii) above and at some
point in this range blade peak suction has reduced and tip flow velocity
increased sufficiently for both surface and vortex cavitation to occur
simultaneously.

(iv) For values of λ around 0.17 the flow through the tip clearance has
become fully turbulent and probably the magnitude of the clearance flow velocity
reaches a maximum about this value.   Incidence has continued to decrease and
the suction peak on the blade has reduced and its location moved further back
along the chord.   The tip flow is now strong enough to produce a vortex of
which the core cavitates before the surface of the blade.   The cavitation
number will, therefore, increase above that in (iii).

(v) For values of λ above about 0.17 the behaviour of the cavitation
curves becomes more problematical due to the increasing uncertainty of the
relative magnitude of the various factors affecting them.   Certainly incidence
continues to decrease and is higher at the lower values of flow coefficient.
Also the static pressure rise through the blade row is much higher at the lower
flow coefficients and this together with the higher incidence could cause the
vortex core to move into a higher static pressure region with a consequent drop
in cavitation number.   At the higher flow coefficients, the much lower static
pressure rise, the vortex being closer to the blade surface and therefore more
influenced by lower blade surface pressures and the fact that the maximum tip
flow velocity has moved back behind the maximum thickness section of the tip
might well cause an overall increase in cavitation number.

(vi) The general reduction of cavitation number with increasing flow
coefficient at constant tip clearances merely reflects the fact that in the
design of the blading of this particular pump no allowance was made for axial
velocity decrement in the wall boundary layer.   This results in smaller
incidences and therefore lower cavitation numbers with increasing values of
flow coefficient.

34. Although the foregoing argument cannot be regarded as conclusive, the
experimental data obtained does tend to support it and if it is correct its
implications are of great importance.   The significance lies in the fact that
for a given blading geometry, a minimum cavitation number exists which is in
fact equal to the blade surface cavitation number as determined solely by
section shape and main flow condition such as incidence.   True, the actual
value of incidence is affected by the tip flow and induced velocities from
the rest of the blade but they will almost always act so as to reduce incidence
which in turn reduces peak suctions so that the actual cavitation number
obtained will be lower than that calculated.   The problem of designing pumps,
therefore, with as low a value of tip cavitation number as possible, reduces to
one of designing the tip section for low peak sections which is exactly the
same procedure as used for delaying surface cavitation further down the blade.
In other words, in a properly designed pump, blade surface and not tip clearance
cavitation still provides the limiting cavitation number.   Usually the
boundary-layer thickness on the duct wall will be much thicker than the critical
tip clearance so that the main practical difficulty in reducing cavitation
number will be in reducing to an optimum value - fixed by the section geometry -
the high incidences due to the axial velocity decrement in the boundary layer.
The smaller the tip clearance below the critical value of λ equal to 0.1,
the greater will be the difficulties in achieving this.   In most cases,
therefore, a tip clearance corresponding to a value of λ of about 0.1 will
probably prove to be the optimum.

Conclusions

35. The variation of tip clearance cavitation number with both tip
clearance and flow coefficient have been obtained.   For the particular

combination of wall boundary layer profile and blade design tested, the following conclusions can be drawn:-

(i) Except possibly at the very highest flow coefficients obtainable, there exists a minimum cavitation number for all values of flow coefficient which occurs at the same value of tip clearance. The non-dimensional value of this optimum tip clearance was found to be between about 0.09 and 0.105 and is related to the critical Reynolds number for the flow through the tip clearance.

(ii) For tip clearances below the optimum value, cavitation first appeared as surface cavitation on the tip section profile.

(iii) For tip clearances above the optimum, vortex cavitation due to the flow through the tip clearance appears first.

36. Conclusions (ii) and (iii) above are applicable to all blading designs and it is likely that a minimum cavitation number is always obtained although the value of tip clearance at which it occurs may vary. The fact that the value of the optimum tip clearance as shown in Figs.11, 12 and 13 appears to be independent of pump R.P.M. and flow coefficient is not yet fully understood. If this value of tip clearance was determined solely by the critical Reynolds number of the flow through it, there would be a significant variation in its value between the curves of Figs.11, 12 and .13. It seems likely, therefore, that it is also dependent on a second parameter which might possibly be a function of the wall boundary layer such as the thickness of the laminar sub-layer. Further work is necessary to clarify this point but it is significant that the value of the optimum tip clearance obtained agrees very closely with that obtained in Ref.2.

37. Tip clearance cavitation number is not the limiting cavitation number in an axial flow pump. In a properly designed unit tip clearance cavitation number reduces to the tip section surface cavitation number and there is no reason why this should not be reduced to a value commensurate with the rest of the blade surface cavitation number.

38. For maximum cavitation resistance the blade clearances in a pump should correspond to values of λ around 0.10. The wall boundary layer profile and blade tip section parameters should be adjusted so that the resultant flow incidence to the tip gives a minimum blade peak suction at the design flow coefficient.

39. Future work

(i) Although the experimental evidence obtained strongly supports the present hypothesis, complete proof is still required. To do this, further instrumentation will be required for detailed flow visualisation studies and for local flow measurements in the tip region of a blade.

(ii) Further experimental investigations directed towards a better understanding of the factors affecting the value of the optimum tip clearance.

(iii) In spite of the fact that tip clearance and blade surface cavitation number have been put in their correct perspective, it is not yet possible to calculate accurately the magnitude of the minimum cavitation inception number. If the three-dimensional effects of clearance flow and interference from the rest of the blading on the tip incidence are ignored, a pessimistic value of inception number will be obtained. A theoretical treatment of the secondary flows in conjunction with the results of the experimental work in (i) and (ii) above will be necessary for this purpose.

References

No.	Author(s)	Title, etc.
1	Dean A. Rains	Tip clearance flows in axial flow compressors and pumps. C.I.T. Report No.5, June, 1954.
2	A. R. Howell	The present basis of axial flow compressor design. R. & M. No.2095. June, 1942.
3	A. R. Howell	Fluid dynamics of axial compressors. The Instit. of Mech. Eng. Proc. 1945. Vol.153.
4	A. D. S. Carter and A. F. Hounsell	General performance data for aerofoils having C.1, C.2 or C.4 base profiles on circular arc camber lines. Unpublished M.o.A. Report.
5	R. A. Jeffs, A. F. Hounsell and R. G. Adams	Further performance data for aerofoils having, C.1, C.2 or C.4 base profiles on circular arc camber lines. Unpublished M.o.A. Report.

Table I/

Table I

Rotor Blades No. of Blades: 13	Section Radius - in.						
	3.000	3.125	3.813	4.500	5.188	5.875	6.000
Circular arc camber line; base profile:- C.5							
Chord - in.	2.42	2.42	2.42	2.42	2.42	2.42	2.42
t/c - Thickness/chord	0.10			0.08			0.06
s/c - Pitch/chord	0.60	0.625	0.763	0.90	1.037	1.175	1.200
V_a/U_m - Flow coefficient				0.80			
ε - Fluid deflection-deg.	48.6	45.4	30.7	20.8	14.2	10.1	9.4
α_1' - Blade inlet angle -deg.	46.8	46.0	49.6	52.4	56.2	59.5	60.0
θ - Camber angle - deg.	66.6	61.1	43.7	30.0	22.4	17.8	16.3
ξ - Stagger angle - deg.	-13.5	-15.5	-27.8	-37.4	-45.0	-50.6	-51.9

Table II

Stator Blades No. of Blades: 13	Section Radius - in.						
	3.000	3.125	3.813	4.500	5.188	5.875	6.000
Circular arc camber line; C.5 base profile							
Chord - in.	2.25	2.25	2.25	2.25	2.25	2.25	2.25
t/c - Thickness/chord	0.06			0.08			0.10
ε - Fluid defl. - deg.	44.6	43.4	37.9	33.4	29.8	26.7	26.3
α_3' - Blade inlet angle - deg.	45.6	44.4	38.9	36.4	34.8	33.7	35.3
θ - Camber angle - deg.	55.5	54.3	48.7	46.6	45.4	44.9	47.2
ξ - Stagger angle - deg.	-17.8	-17.2	-14.5	-13.1	-12.1	-11.2	-11.7

Table III

Blade Tip Clearance in.	λ	Pump R.P.M.	Axial Velocity V_a ft/sec	$\dfrac{V_a}{U_m}$	Cavitation Pressure (P_c) lbs/sq ft absolute	$K_{va} = \dfrac{P_c - P_v}{\frac{1}{2}\rho V_a^2}$
0.0055	0.0378	600	18.74	0.794	623	1.83
		675	21.55	0.806	801	1.78
		750	23.60	0.800	1052	1.95
		600	17.58	0.745	873	2.91
		675	19.90	0.745	1043	2.73
		750	22.10	0.749	1609	3.39
		600	16.58	0.702	1126	4.21
		668	18.28	0.692	1764	5.45
		750	20.65	0.700	2344	5.66
		600	19.90	0.843	622	1.62
		678	22.70	0.846	751	1.50
		750	25.00	0.846	869	1.43
		600	20.93	0.886	590	1.39
		675	23.82	0.892	695	1.26
0.010	0.0688	600	16.60	0.702	1421	5.35
		675	18.60	0.696	2026	6.04
		750	20.60	0.698	2580	6.25
		600	21.00	0.890	628	1.47
		675	23.65	0.885	775	1.43
		750	26.35	0.894	933	1.38
		675	23.10	0.865	732	1.416
		600	20.55	0.870	570	1.39
		750	25.64	0.870	814	1.27
		600	19.50	0.826	530	1.44
		675	21.98	0.824	657	1.40
		750	24.32	0.824	888	1.55
		597	18.76	0.798	611	1.79
		675	21.38	0.800	690	1.56
		750	23.50	0.796	822	1.54
		600	17.58	0.745	704	2.37
		675	19.90	0.745	783	2.03
		750	22.08	0.749	1856	3.91
0.018	0.124	675	23.02	0.863	707	1.37
		600	20.56	0.870	599	1.46
		750	25.65	0.870	798	1.25
		600	19.35	0.820	569	1.57
		675	22.10	0.828	731	1.54
		675	23.28	0.872	783	1.49
		750	24.25	0.822	862	1.51
		597	18.80	0.799	650	1.90
		675	21.45	0.803	735	1.65
		750	23.50	0.796	800	1.49
		600	17.60	0.746	700	2.34
		675	19.90	0.745	803	2.09
		750	22.02	0.746	1084	2.30
		600	16.60	0.702	863	3.27
		675	18.60	0.696	1252	3.73
		750	20.60	0.698	1473	3.57
		600	21.10	0.894	680	1.58
		675	23.85	0.894	781	1.42
		750	26.45	0.897	903	1.33
0.026	0.179	600	21.70	0.920	779	1.70
		675	23.95	0.896	880	1.58
		750	26.30	0.891	986	1.47
		600	20.80	0.881	756	1.80
		600	20.05	0.849	747	1.92
		675	22.68	0.849	811	1.63
		750	25.55	0.866	996	1.58
		600	18.80	0.796	730	2.13

Table III (contd.)

Blade Tip Clearance in.	λ	R.P.M.	Axial Velocity V_a ft/sec	$\dfrac{V_a}{U_m}$	Cavitation Pressure (P_c) lbs/sq ft absolute	$K_{va} = \dfrac{P_c - P_v}{\frac{1}{2}\rho V_a^2}$
0.026	0.179	675	21.55	0.806	856	1.90
		750	23.70	0.804	1103	2.02
		750	22.20	0.752	1721	3.60
		675	19.95	0.746	1279	3.31
		597	17.80	0.756	865	2.84
		600	16.57	0.702	1450	5.45
		675	18.60	0.696	1823	5.43
		750	20.80	0.705	2359	5.62
0.010	0.0688	675	21.74	0.814	676	1.48
0.039	0.268	600	16.75	0.709	1460	5.36
		675	18.75	0.702	2081	6.10
		750	20.85	0.706	2451	5.81
		750	22.20	0.752	1536	3.21
		675	20.00	0.749	1042	2.69
		600	17.70	0.749	925	3.05
		600	18.70	0.792	833	2.46
		675	21.60	0.809	899	1.99
		750	23.70	0.803	1065	1.96
		750	25.05	0.850	1061	1.74
		675	22.55	0.844	836	1.70
		600	20.05	0.849	820	2.10
		600	21.3	0.902	847	1.93
		675	24.0	0.899	897	1.61
		750	26.35	0.893	1042	1.55
0.057	0.392	600	21.28	0.902	797	1.81
		675	24.22	0.906	1052	1.85
		750	27.00	0.915	1296	1.83
		600	20.07	0.851	859	2.20
		675	22.80	0.854	996	1.97
		750	25.35	0.859	1238	1.99
		600	18.75	0.794	830	2.44
		675	21.55	0.806	1015	2.26
		750	23.70	0.804	1236	2.26
		750	22.10	0.749	1377	2.90
		675	19.95	0.746	1112	2.88
		597	17.70	0.752	908	2.99
		603	16.60	0.700	1067	3.99
		675	18.70	0.700	1312	3.87
		750	20.77	0.704	1634	3.91
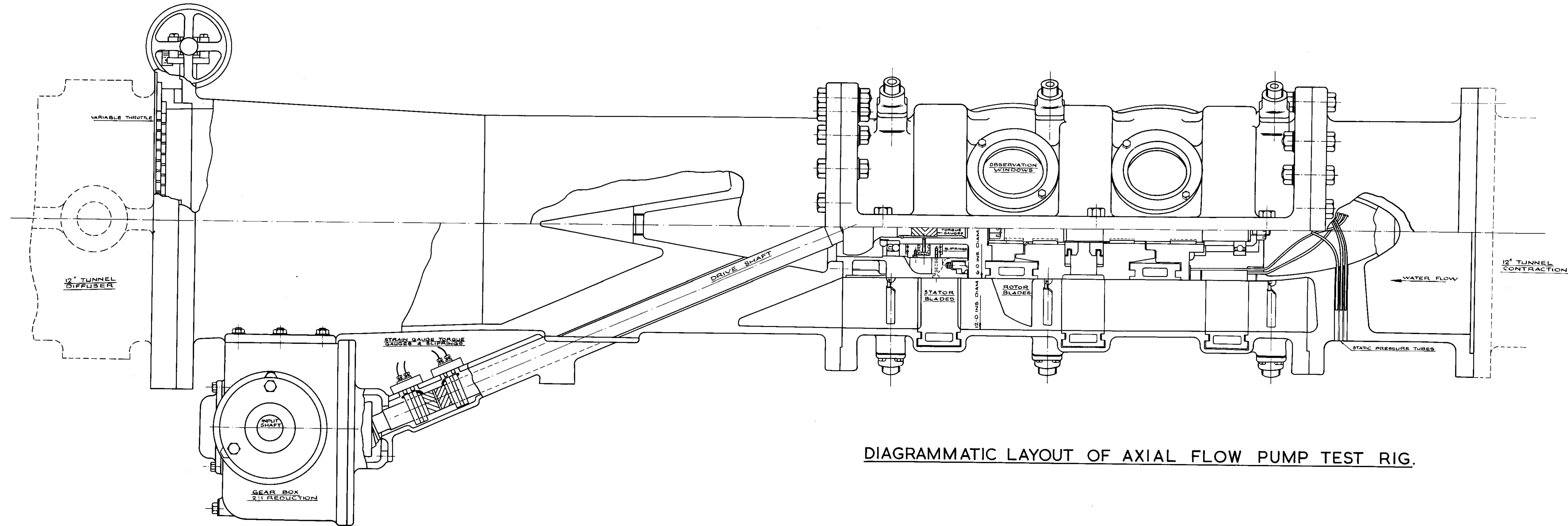
DIAGRAMMATIC LAYOUT OF AXIAL FLOW PUMP TEST RIG.

VARIABLE THROTTLE

12" TUNNEL DIFFUSER

12" TUNNEL CONTRACTION

WATER FLOW

OBSERVATION WINDOWS

DRIVE SHAFT

TORQUE GAUGES

SLIPRINGS

STATOR BLADES

ROTOR BLADES

12.0 INS DIAM

9.0 INS DIAM

STATIC PRESSURE TUBES

STRAIN GAUGE TORQUE GAUGES & SLIPRINGS

INPUT SHAFT

GEAR BOX 2:1 REDUCTION

A.R.L/RI/G/HY/11/2

FIG. I

$\frac{3}{32}$" DIA.

$\frac{9}{64}$"

0·053"

0·004"

0·022"
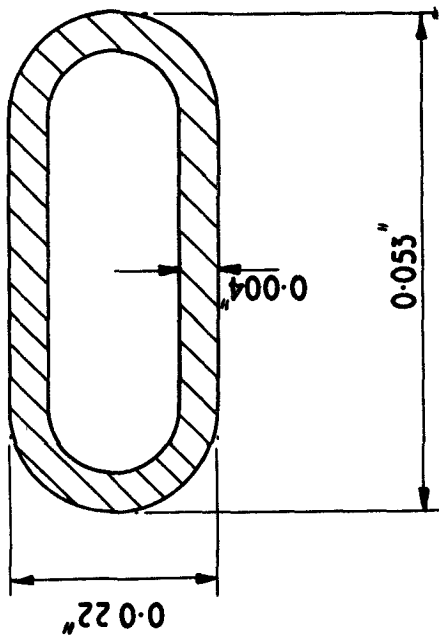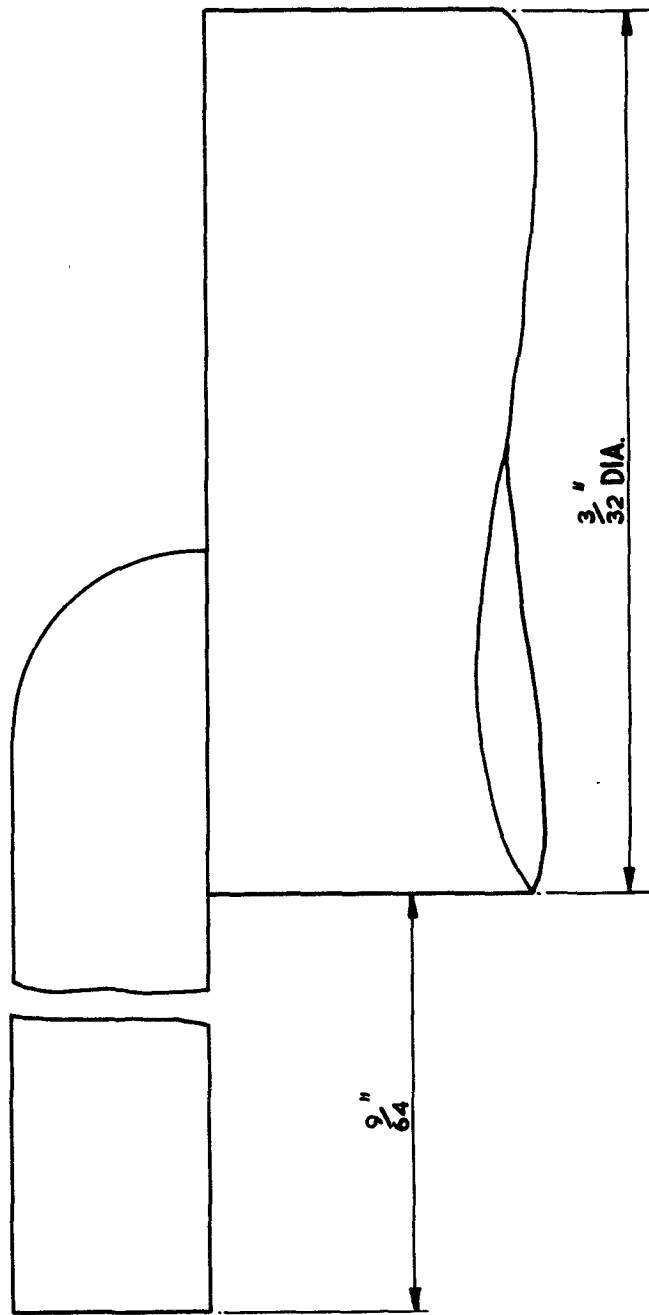
BOUNDARY LAYER PITOT TUBE.

FIG. 2

CAVITATION INCEPTION RESULTS FOR $\lambda = \cdot 0378$.
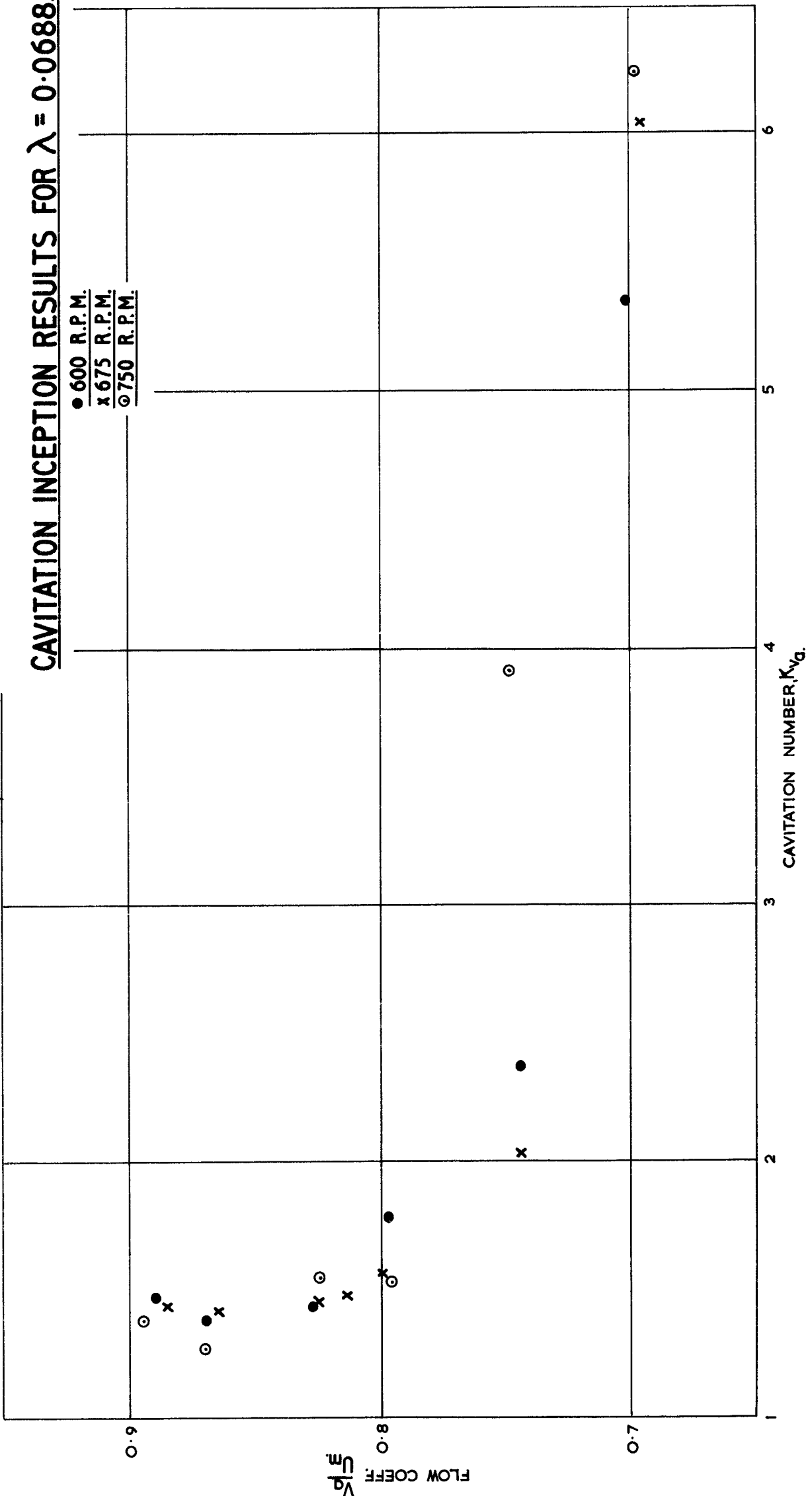
● 600 R.P.M.
X 675 R.P.M.
⊙ 750 R.P.M.

CAVITATION NUMBER, K_{v_a}.

FLOW COEFF $\frac{V_a}{U_m}$.

FIG. 3

CAVITATION INCEPTION RESULTS FOR λ = 0·0688.

● 600 R.P.M.
x 675 R.P.M.
⊙ 750 R.P.M.

FLOW COEFF $\frac{V_a}{U_m}$

CAVITATION NUMBER, K_{V_a}

FIG. 4

FIG. 5

CAVITATION INCEPTION RESULTS FOR λ=0·124

● 600 R.P.M.
X 675 R.P.M.
⊙ 750 R.P.M.

FLOW COEFF. $\frac{V_a}{U_m}$

0·9

0·8

0·7

CAVITATION NUMBER, K_{V_a}

1   2   3   4   5   6
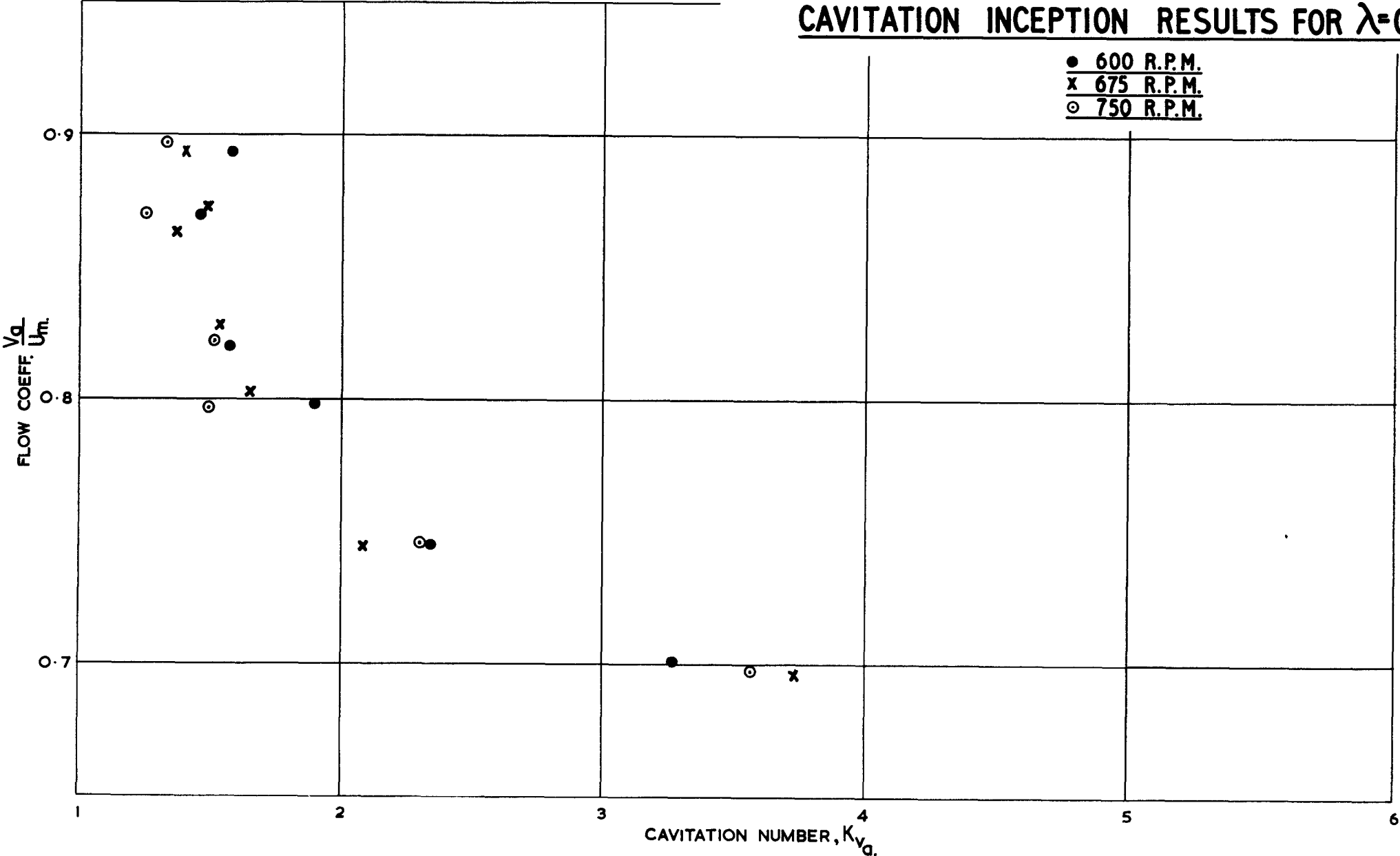
CAVITATION INCEPTION RESULTS FOR λ = 0.179

● 600 R.P.M.
× 675 R.P.M.
⊙ 750 R.P.M.
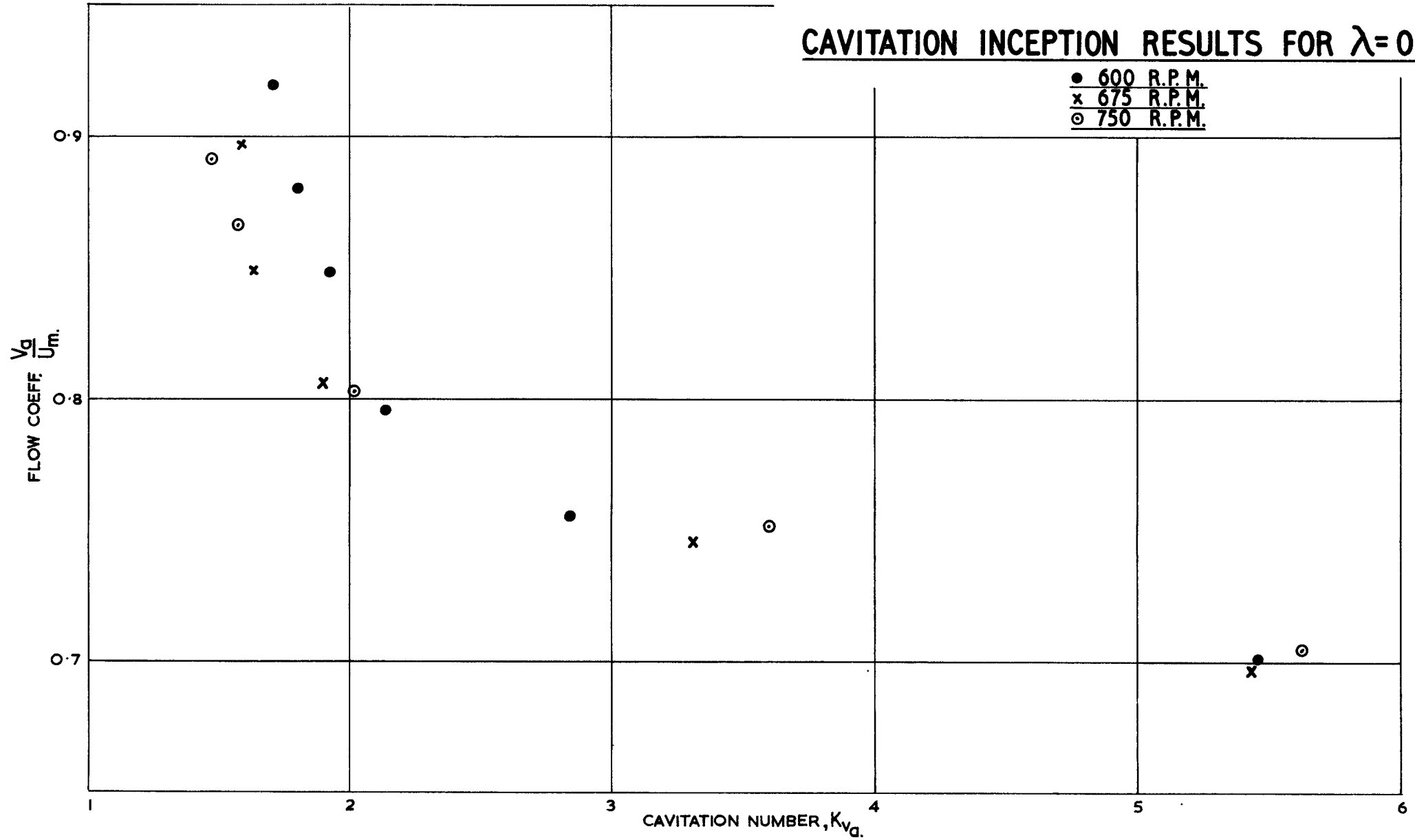
FIG. 6

CAVITATION INCEPTION RESULTS FOR $\lambda = 0.268$

● 600 R.P.M.
X 675 R.P.M.
⊙ 750 R.P.M.

FLOW COEFF, $\frac{V_a}{U_m}$

CAVITATION NUMBER, K_{v_a}
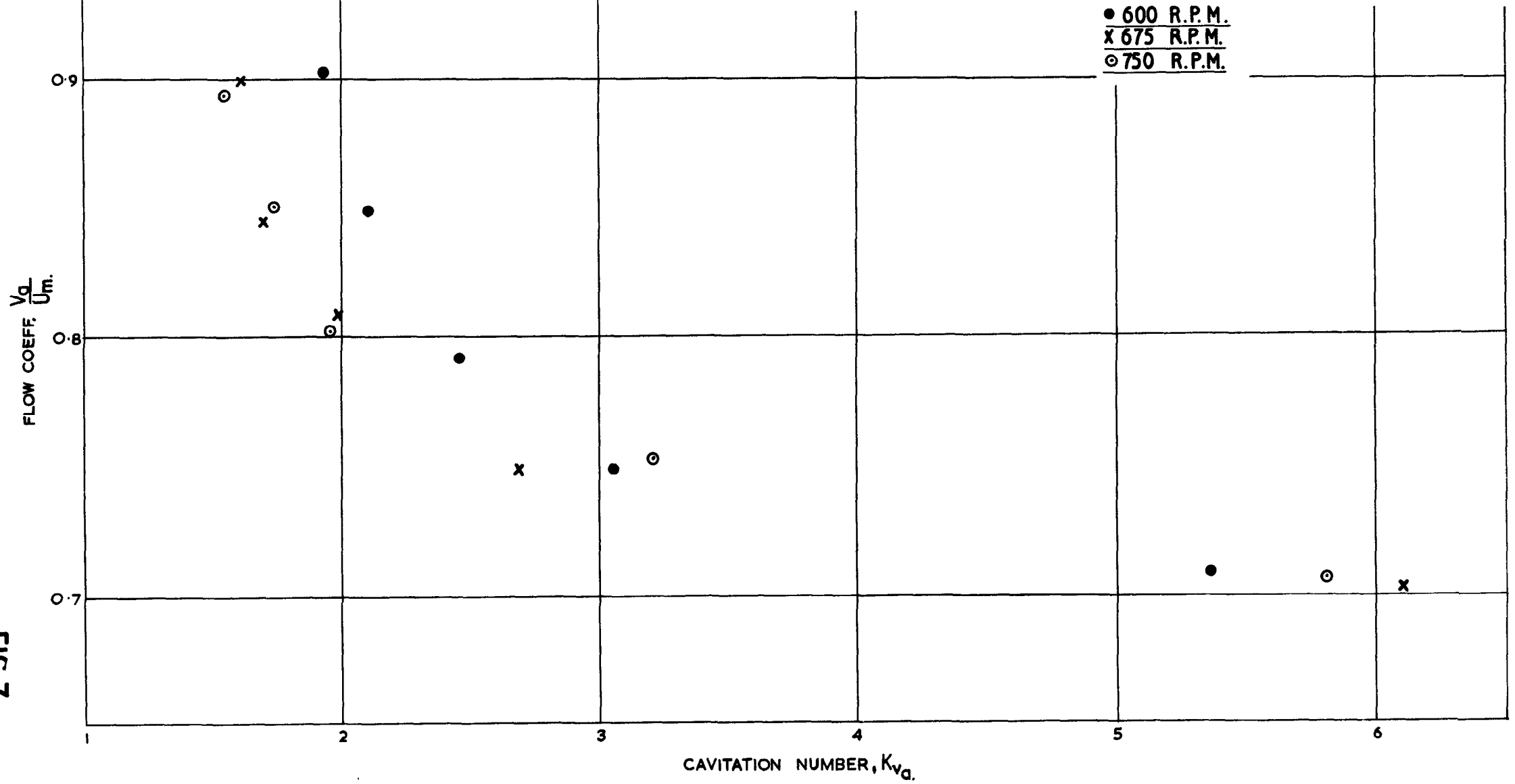
FIG.7

CAVITATION INCEPTION RESULTS FOR $\lambda = 0.392$

● 600 R.P.M.
X 675 R.P.M.
⊙ 750 R.P.M.
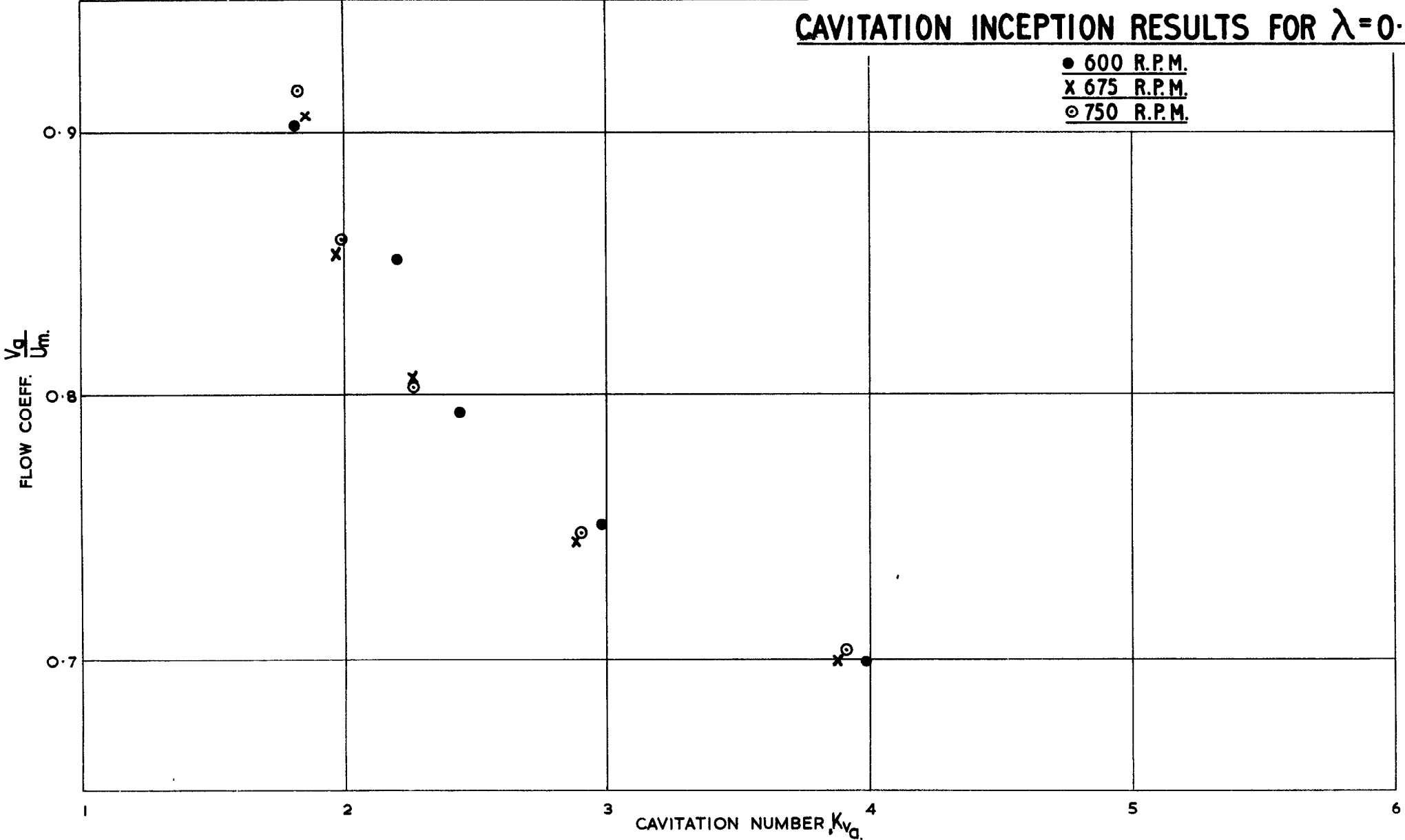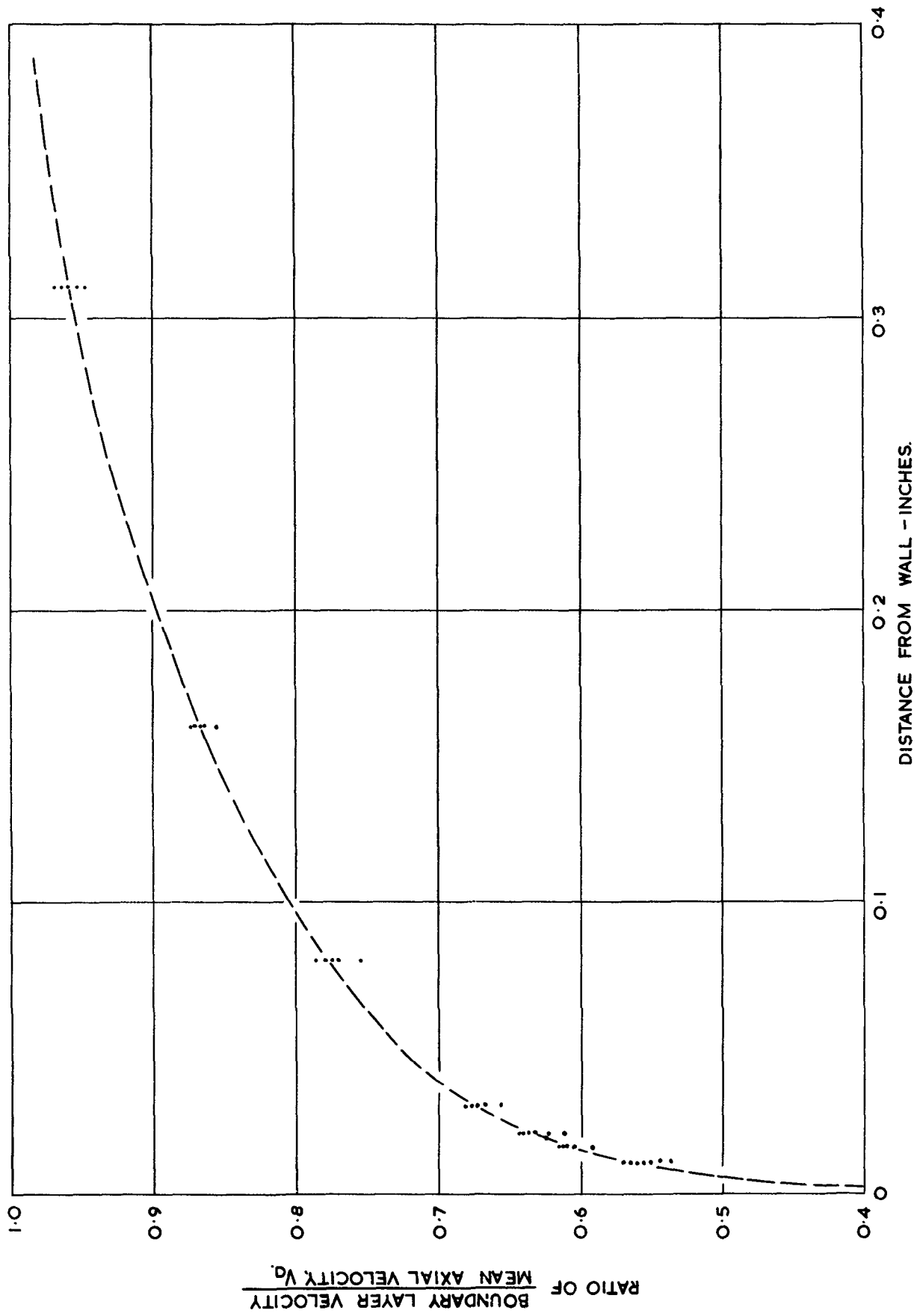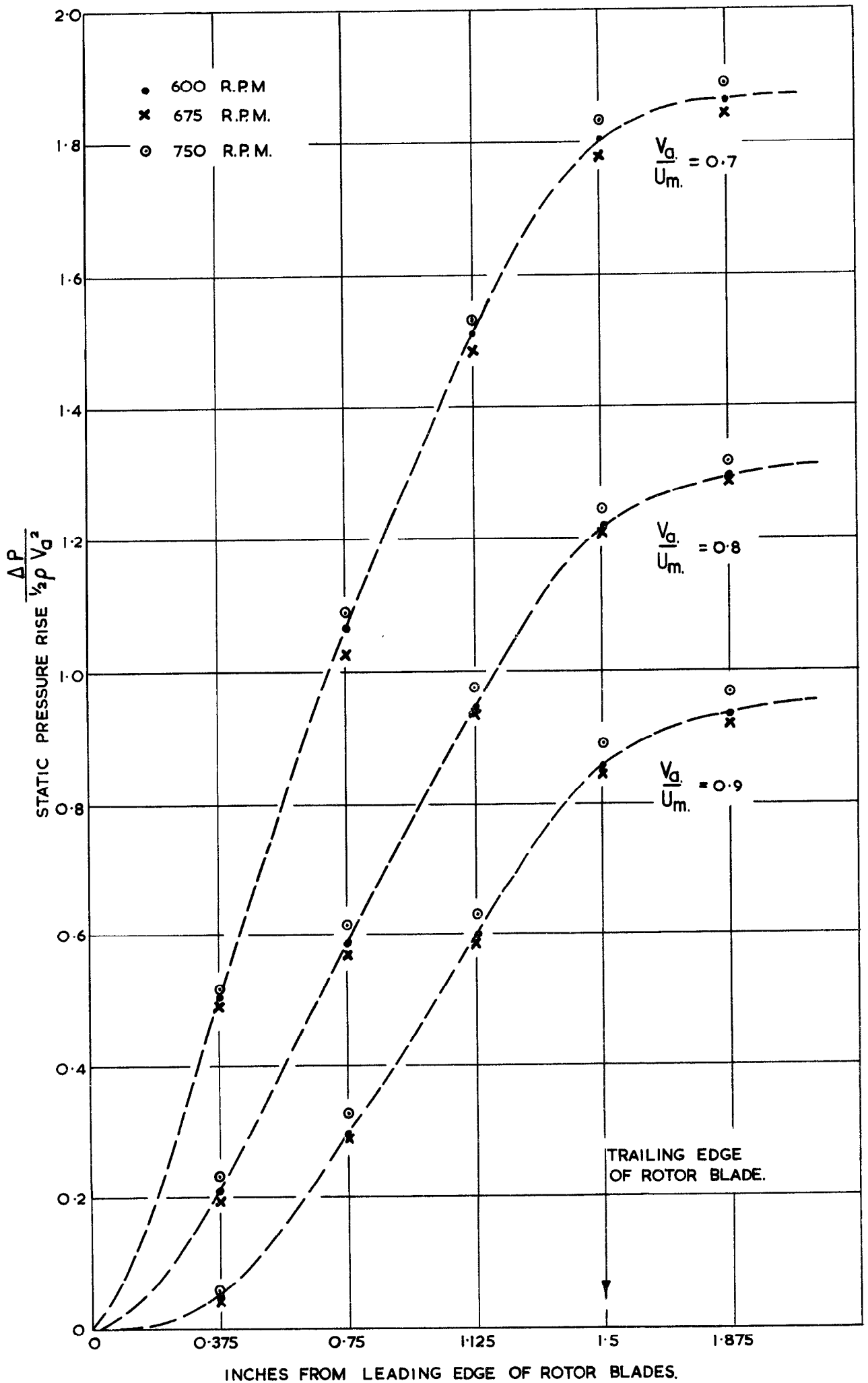
FLOW COEFF. $\frac{V_a}{U_m}$

CAVITATION NUMBER, K_{V_a}

FIG. 8

WALL BOUNDARY LAYER PROFILE.

FIG.9

STATIC PRESSURE RISE
ACROSS ROTOR BLADES.

FIG.10

FIG. II

K_{V_a} VERSUS λ.

R. P. M. CONSTANT AT 600.

X INTERPOLATED POINTS FROM FIGS 3-8.

CAVITATION INCEPTION NUMBER - K_{V_a}.

NON - DIMENSIONAL TIP CLEARANCE - λ.

$\dfrac{V_a}{U_m}$.

0·70

0·75

0·80

0·85

0·90

FIG. 12.

$\underline{K_{V_a}}$ VERSUS λ.

R.P.M. CONSTANT AT 675.
X INTERPOLATED POINTS FROM FIGS 3-8.

$\dfrac{V_a}{U_m}$

0·7
0·75
0·80
0·85
0·90

CAVITATION INCEPTION NUMBER - K_{V_a}

NON-DIMENSIONAL TIP CLEARANCE - λ.
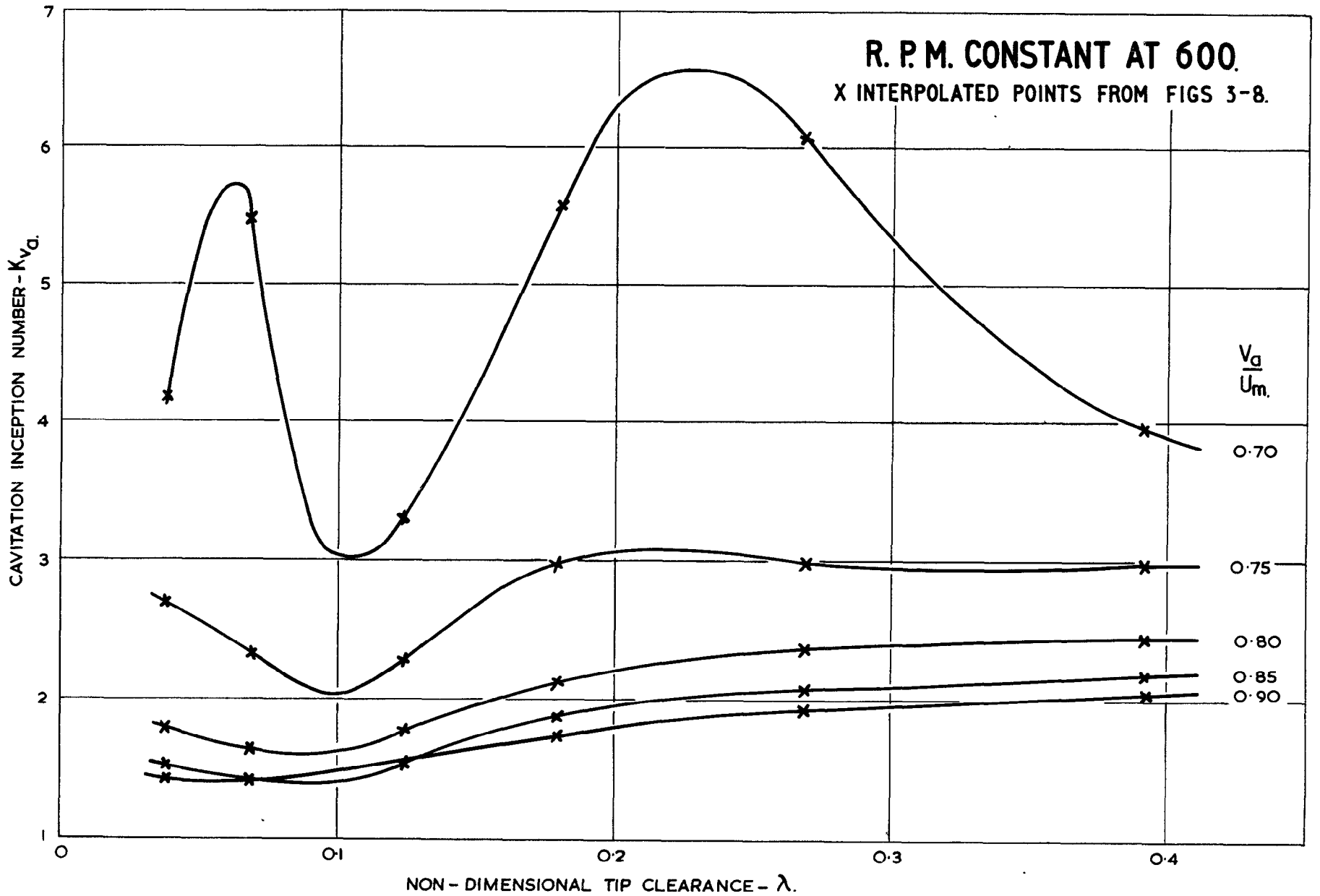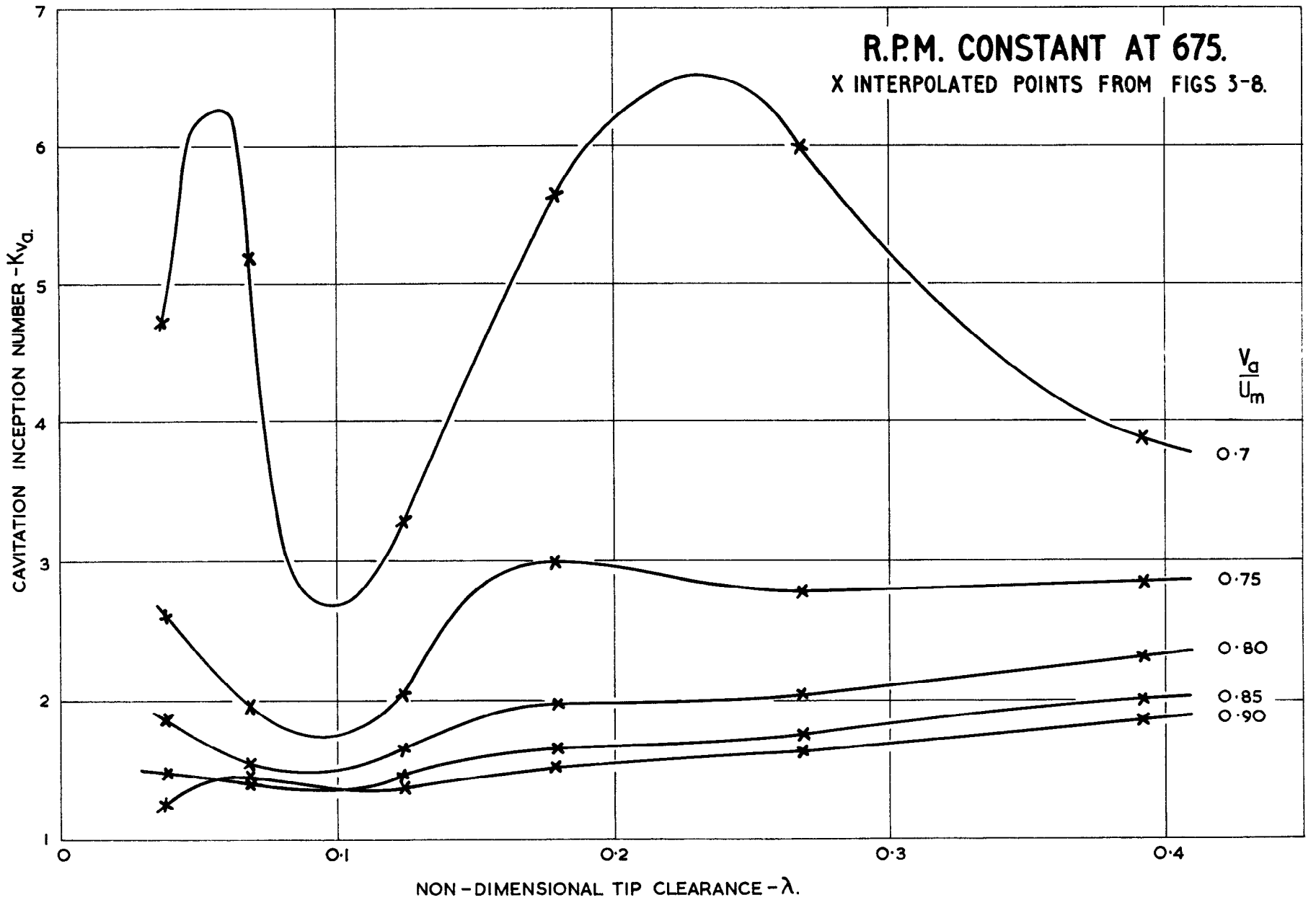
R.P.M CONSTANT AT 750.
X INTERPOLATED POINTS FROM FIGS. 3-8.

$\dfrac{V_a}{U_m}$

0·7

0·75

0·80

0·85

0·90

NON-DIMENSIONAL TIP CLEARANCE – λ.

CAVITATION INCEPTION NUMBER – K_{V_a}.

K_{V_a} VERSUS λ.
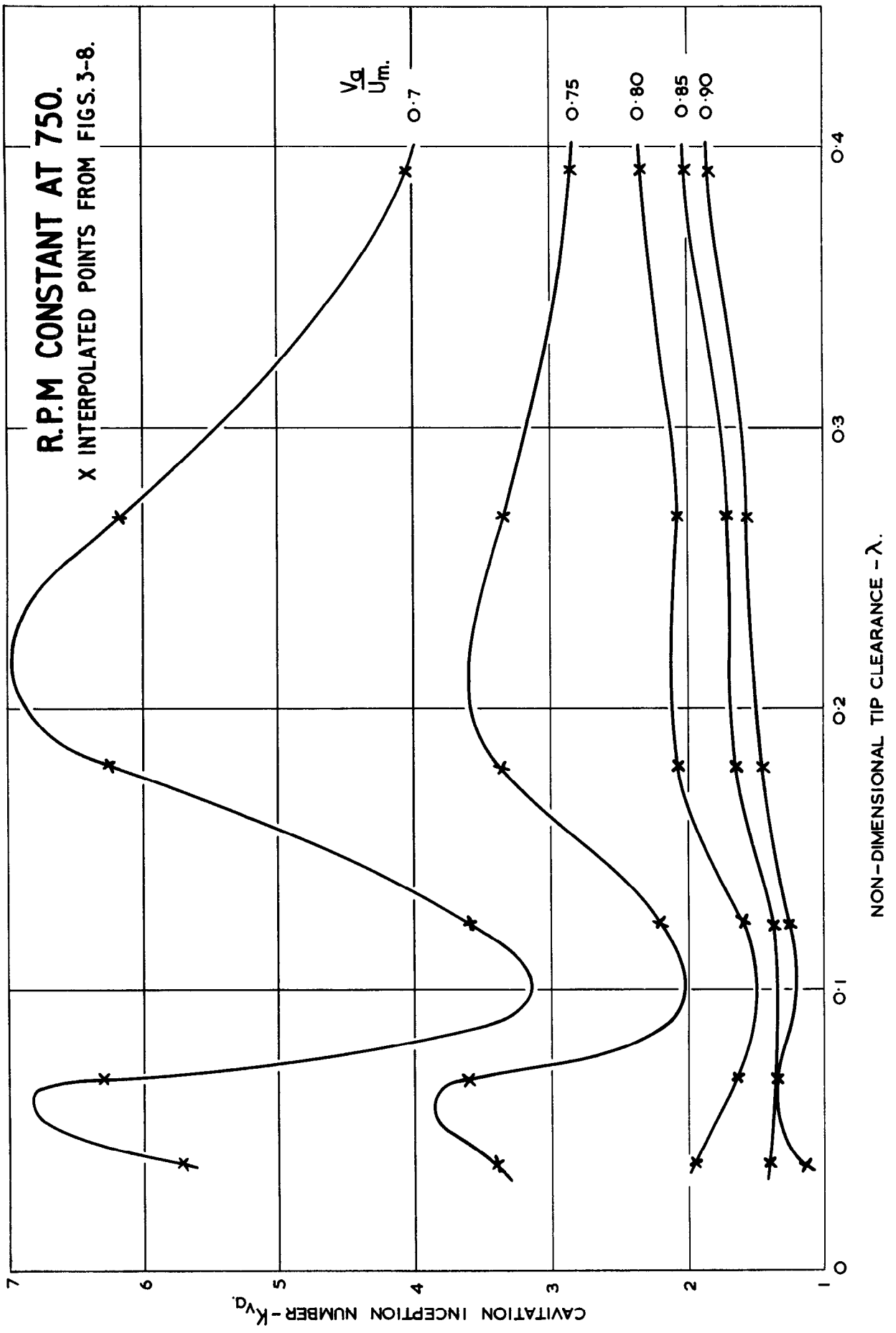
FIG.13
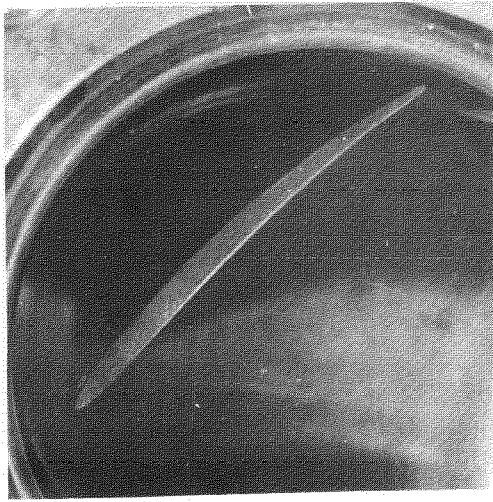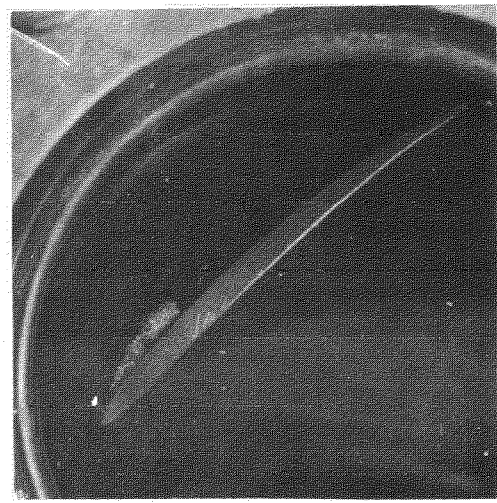
(a) $\lambda = \cdot0378$ $\dfrac{V_a}{U_m} = 0.7$ $K_{V_a} \simeq 4.7$
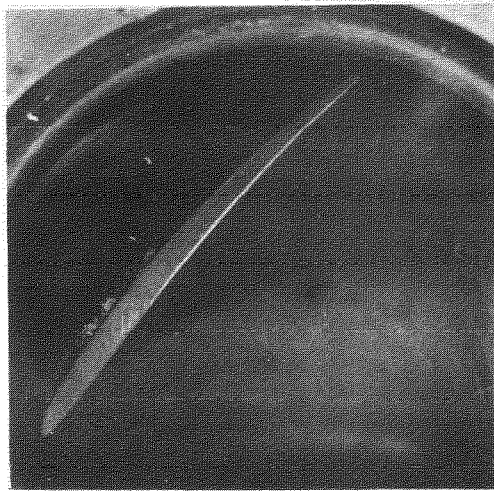
(b) $\lambda = \cdot0378$ $\dfrac{V_a}{U_m} = 0.8$ $K_{V_a} \simeq 1.85$

(c) $\lambda = \cdot0378$ $\dfrac{V_a}{U_m} = 0.9$ $K_{V_a} \simeq 1.25$
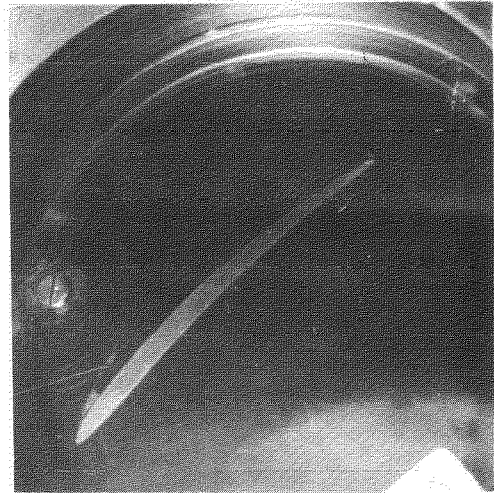
(d) $\lambda = \cdot0688$ $\dfrac{V_a}{U_m} = 0.7$ $K_{V_a} \simeq 5.2$
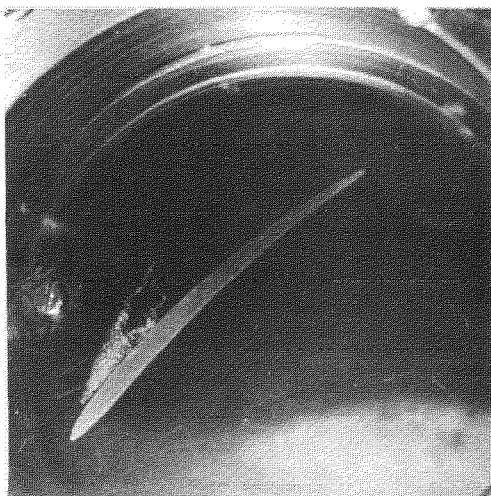
(e) $\lambda = \cdot0688$ $\dfrac{V_a}{U_m} = 0.75$ $K_{V_a} \simeq 1.95$
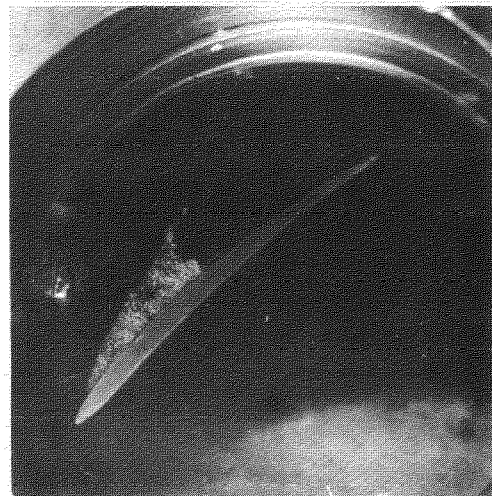
(f) $\lambda = \cdot0688$ $\dfrac{V_a}{U_m} = 0.8$ $K_{V_a} \simeq 1.56$
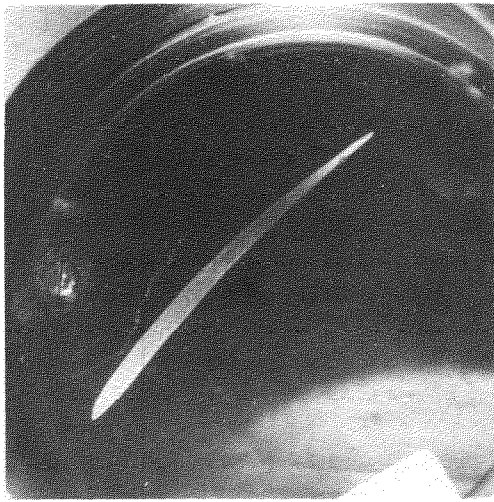
(g) $\lambda = \cdot 0688$

$\dfrac{V_a}{U_m} = 0.9$ $K_{V_a} \simeq 1.45$
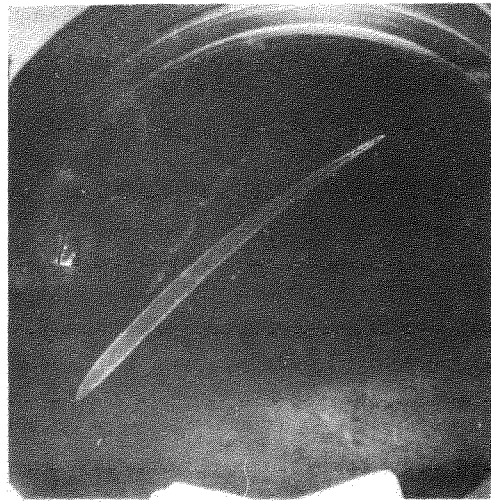
(h) $\lambda = 0.124$

$\dfrac{V_a}{U_m} = 0.7$ $K_{V_a} \simeq 3.3$

(j) $\lambda = 0.124$

$\dfrac{V_a}{U_m} = 0.8$ $K_{V_a} \simeq 1.66$
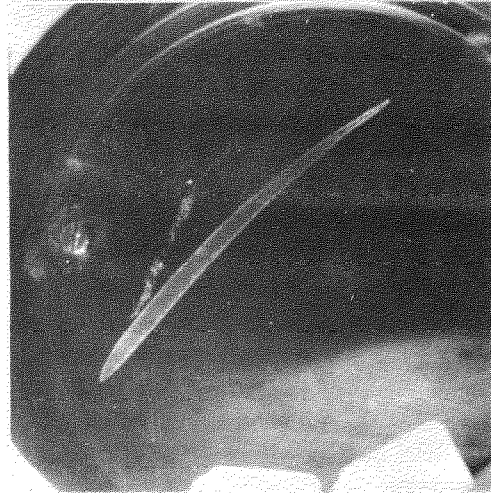
(k) $\lambda = 0.124$

$\dfrac{V_a}{U_m} = 0.8$ $K_{V_a} \simeq 1.66$
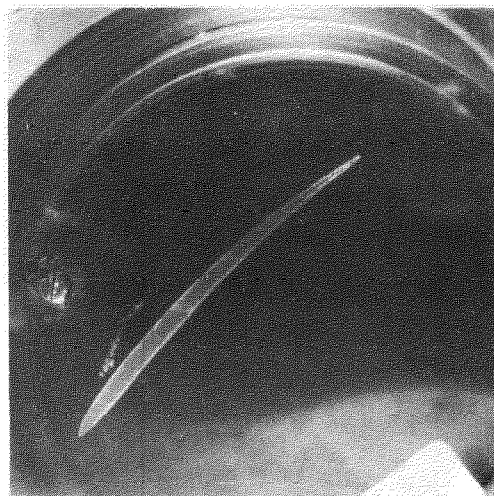
(l) $\lambda = 0.124$

$\dfrac{V_a}{U_m} = 0.9$ $K_{V_a} \simeq 1.38$
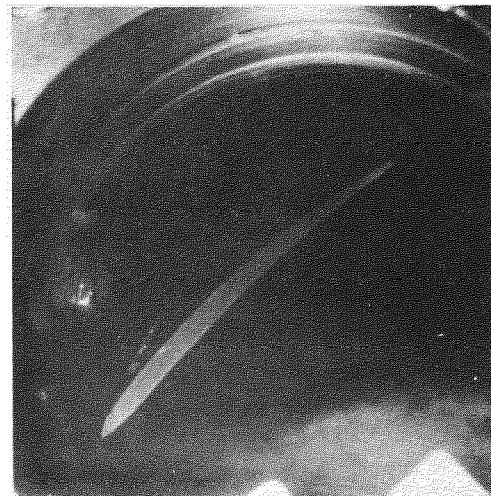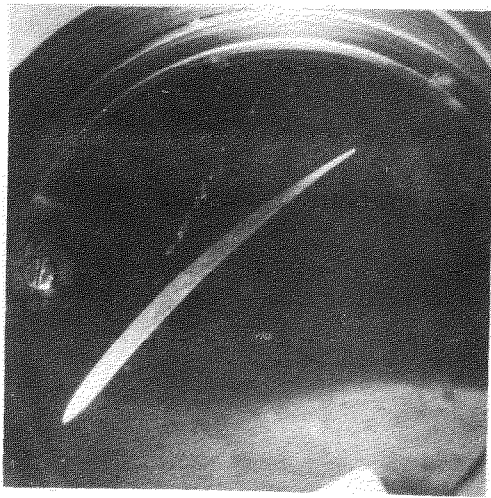
(m) $\lambda = 0.179$
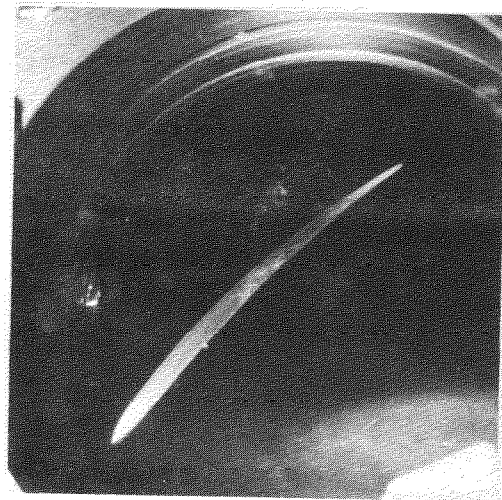
$\dfrac{V_a}{U_m} = 0.7$ $K_{V_a} \simeq 5.65$
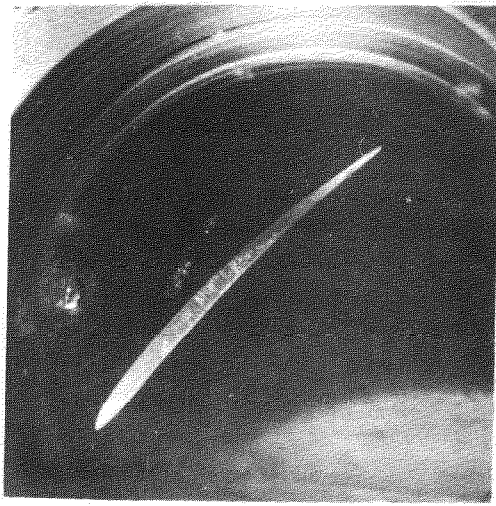
(n) $\lambda = 0.179$
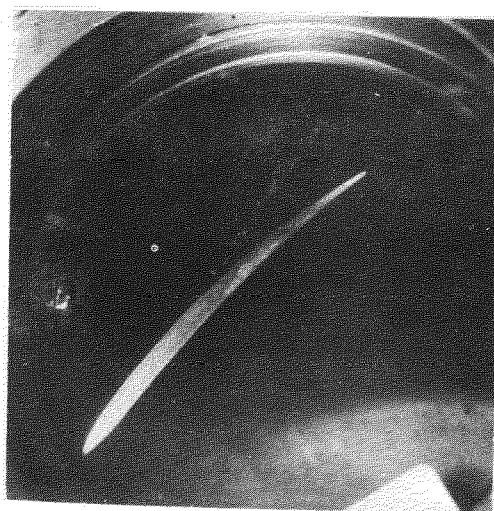$\dfrac{V_a}{U_m} = 0.8$ $K_{V_a} \simeq 1.98$
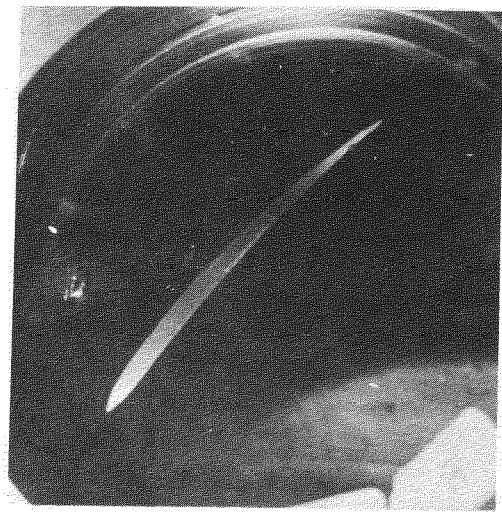
(O) $\lambda = 0.179$
$\dfrac{V_a}{U_m} = 0.9$ $K_{V_a} \simeq 1.52$

(P) $\lambda = 0.392$
$\dfrac{V_a}{U_m} = 0.7$ $K_{V_a} \simeq 3.9$

(q) $\lambda = 0.392$
$\dfrac{V_a}{U_m} = 0.8$ $K_{V_a} \simeq 2.3$

(r) $\lambda = 0.392$
$\dfrac{V_a}{U_m} = 0.9$ $K_{V_a} \simeq$

PUMP R.P.M. = 675

C.P.No. 527

C.P.No. 527